

Relativistic electronic structure of the Sr₂ molecule

Svetlana Kotochigova^{a)}

Department of Physics, Temple University, Philadelphia, Pennsylvania 19122-6082, USA

(Received 7 August 2007; accepted 1 November 2007; published online 9 January 2008)

Diatomic Sr₂ has been proposed as a good candidate for precision measurement of possible time variation of fundamental constants. Precise knowledge of its vibrational structure and Stark shift of its levels in an optical lattice is required for realization of this proposal. Motivated by these ideas we have performed a numerical calculation of interatomic potentials and transition dipole moments of the Sr₂ molecule using an *ab initio* relativistic configuration interaction valence bond self-consistent-field method. © 2008 American Institute of Physics. [DOI: 10.1063/1.2817592]

I. INTRODUCTION

Cold strontium molecules are proposed for precision measurements of possible time variation of fundamental physical constants.¹ The binding energy of a rovibrational state is sensitive to the reduced mass of the molecule and, thus, a measurement of the energy difference between a weakly and a strongly bound vibrational level becomes very sensitive to the temporal variation of the electron-proton mass ratio.

In the proposed experiment ultracold Sr₂ dimers will be confined in an optical lattice to avoid intermolecular interactions. Crucial concern, however, is the effect of the trapping potential on the vibrational levels. It is reasonable to expect that Stark shifts are different for weakly and deeply bound vibrational levels. The main property relevant to Stark shifts is molecular dynamic polarizability as a function of lattice frequency and vibrational quantum number. Calculation of polarizability of various vibrational levels requires accurate determination of interatomic potentials and transition dipole moments. Moreover, the realization of the proposal¹ will require substantial experimental and theoretical efforts to provide accurate information on the rovibrational structure of ground and excited state potentials and Franck-Condon factors between them. Our theoretical study is a part of these efforts as a starting point for the description of molecular properties.

The first laser experiments with alkaline-earth dimers have been stimulated by the fact that they have a shallow van der Waals ground state and deeply bound excited states. The observation and theoretical analysis of laser-excited photoluminescence of the Sr₂ dimer has been reported in Ref. 2. The photoluminescence spectrum was found to contain both discrete molecular lines and strong continua. Authors have associated the observed molecular spectra with emission from the A ¹Σ_u⁺ state into X ¹Σ_g⁺. Computer modeling of the observed spectra was used to obtain Morse potential parameters for both the X ¹Σ_g⁺ ground state ($D_e = 1100 \pm 100$ cm⁻¹) and the A ¹Σ_u⁺ state ($D_e = 5460 \pm 100$ cm⁻¹).

More detailed analysis of laser-induced emission of the Sr₂ dimer has been performed by Gerber *et al.*³ Their spec-

trum contained discrete molecular series at excitation wavelengths from 450 to 600 nm. The analysis of the well resolved discrete fluorescence spectrum led to a set of Dunham coefficients and Rydberg-Klein-Rees (RKR) potentials for X ¹Σ_g⁺ ground and excited A ¹Σ_u⁺ states. The predicted dissociation energy D_e is equal to 1060 cm⁻¹ and the minimum of the potential lies at $R_e = 8.409$ a.u. In spite of the fact that the potential of Ref. 3 is the most precise potential available for the ground state of Sr₂, it is obtained in the restricted range of internuclear separations from 7.2 to 14 a.u. The spectroscopic constants of the excited B ¹Π_u state have been deduced from depletion spectroscopy of Sr₂ B ¹Π_u-X ¹Σ_g⁺ system.⁴

The long-range dispersion potential of the Sr₂ ground state can be constructed using the form $V(R) = D_e - C_6/R^6 - C_8/R^8$, where the C_6 and C_8 coefficients are dispersion parameters. A coupled-cluster effective-Hamiltonian approximation was used in Ref. 5 to calculate the C_6 coefficients for the ground state Sr₂ potential. Numerical values of C_6 were obtained from polarizabilities calculated at imaginary frequencies. The so called polarized sets developed by Sadlej and Urban⁶ have been used for this calculation. These Gaussian sets have been optimized to calculate electrical properties of atoms. The recommended value of C_6 is $3212.3E_h a_0^6$. A relativistic many-body calculation of the C_6 coefficient for the Sr₂ ground state was performed by Porsev and Derevianko.⁷ They apply several theoretical methods to describe most of contributions to the dispersion coefficient. The dominant contribution to C_6 is evaluated with the configuration interaction (CI) method in combination with many-body perturbation theory. The smaller contributions are obtained by applying the relativistic random-phase and Dirac-Hartree-Fock approximations. The value was adjusted with known theoretical and experimental data for electric-dipole matrix elements and transition frequencies. The resulting value of van der Waals coefficient C_6 for Sr₂ was $3170(196)E_h a_0^6$. Reanalyses of the value of Ref. 7 based on a more accurate lifetime of the $5s5p$ ¹P₁ level measured in Ref. 8 predicts $C_6 = 3103(7)E_h a_0^6$.⁹

Boutassetta *et al.*¹⁰ and later Czuchaj *et al.*¹¹ have calculated the ground and lower lying excited triplet and singlet states of Sr₂. In both calculations an *ab initio* nonrelativistic

^{a)}Electronic mail: skotochigova@nist.gov.

multiconfiguration self-consistent-field method has been used. In Ref. 11 an additional multireference second order perturbation theory was applied to obtain better agreement with experimental data for the ground state of Sr₂. Although reasonably good agreements with the RKR potential³ have been reported, there is still a significant discrepancy between the excited state potentials obtained in Refs. 10 and 11.

Collisions between ultracold Sr atoms have also been studied over the past decade. Reference 12 has studied collisions between excited and ground state Sr atoms in a magneto-optical trap based on an allowed ¹S-¹P transition. In Ref. 13 the narrow intercombination line ¹S-³P₁ was used to cool Sr atoms to a temperature of about 400 nK. Photoassociation spectroscopy near the ¹S-¹P transition has been used in Refs. 8 and 14 to determine the *s*-wave scattering length of the ⁸⁶Sr and ⁸⁸Sr isotopes and long-range C₃ coefficients of excited interatomic potentials. Photoassociation near the intercombination line was first achieved by in Ref. 15. Their measurements led to values for the C₃ and C₆ coefficients of potentials dissociating to the ¹S-³P₁ limit.

The purpose of this work is to provide molecular data that can be used to evaluate the feasibility of the cold Sr₂ molecules for high-precision frequency measurements. We apply *ab initio* relativistic configuration interaction valence bond self-consistent-field method to calculate the ground *gerade* and low-excited *ungerade* electronic potentials of Sr₂ as well as their transition dipole moments. Since there is no other data on relativistic excited potentials and transition dipole moments of the Sr₂ molecule available from the literature, we performed a set of calculations with different basis sets to analyze the matching of our theoretical results to the experimental RKR potential for ground X ¹Σ_g⁺ and excited A ¹Σ_u⁺ potentials of Ref. 3. We have chosen to use the basis set that gives the best agreement with experiment. We have also carefully analyzed the long-range parameters C₃, C₆, and C₈ obtained by fitting of our long-range potential to the dispersion formula and comparing them with the published data.^{7,9,15}

The paper is organized as follows. Description of our computational approach is given in Sec. II. Electronic potentials of *gerade* ground state and *ungerade* excited states and a table of molecular constants are presented in Sec. III. Transition dipole moments between the ground X and excited states are described in Sec. IV. Tables of potential energies and transition dipole moments of Sr₂ versus internuclear separation can be found through EPAPS.¹⁶

II. COMPUTATIONAL APPROACH

The basic idea behind the valence bond method is that the electronic molecular wavefunction Φ of the relativistic many electron Hamiltonian \hat{H} is constructed from atomic orbitals of the constituent atoms A and B. In essence, the molecular wavefunction is given by

$$\Phi = \sum_{\alpha} C_{\alpha} \det_{\alpha} \quad (1)$$

where each det is an antisymmetrized (\hat{A}) product of two atomic Slater determinants,

$$\det_{\alpha} = \hat{A}(\det_{\alpha}^A \cdot \det_{\alpha}^B). \quad (2)$$

The variational coefficients C_α in Eq. (1) are obtained by solving a generalized eigenvalue matrix problem. In our approach the det_α are not orthogonal. The relativistic valence bond configuration interaction (RVB-CI) method in its original form is described in more detail in Ref. 17, where it was used to calculate the electronic structure of RbCs molecule.

In this paper we report on development and application of an approach for optimizing atomic orbitals within the context of the relativistic valence bond configuration interaction method. These ideas are based on the method developed in Refs. 18–20 and used in a multiconfigurational self-consistent-field calculations. The optimized orbitals are used to iteratively improve the original Dirac-Fock orbitals and accelerate the CI convergence. It is applicable to the ground as well as to excited states of molecule.

The optimization procedure includes an interactive alternation between the determination of CI coefficients and improvement of the atomic orbitals. First, the CI expansion coefficients are determined from the usual variational principle on the many-electron Slater determinants, constructed from atomic orbitals. The expansion coefficients are determined by the variational method. Subsequently, a single solution Φ₀ with energy E₀ of the CI procedure is chosen. Improved orbitals are then obtained by allowing unitary transformations on the space spanned by the original atomic orbitals, based on the expansion coefficients of the single excited states. These transformations of either orthogonal or nonorthogonal atomic orbitals can be performed by applying an exponential operator on the Slater determinants.

The transformed wavefunction Ψ is

$$\Psi = \Phi_0 + \sum_{i < j} T_{ij} \Phi_0(i \rightarrow j), \quad (3)$$

where the un-normalized Φ₀(i→j) are “singly excited states” relative to the reference state Φ₀, where each appearance of the single electron orbital *i* is replaced by orbital *j*, and the T_{ij} are the elements of the transformation matrix. The generalized Brillouin theorem ⟨Φ₀(i→j)| $\hat{H}-E_0$ |Ψ⟩=0 can be used to find the T_{ij} iteratively. The process converges quickly if the initial choice of orbitals and the CI coefficients are close to the final result.

III. GROUND AND EXCITED POTENTIALS

We create a multiconfiguration basis set for the calculation of the ground state potential of the Sr₂ molecule based on self-consistent Dirac-Fock atomic orbitals belonging to the [1s² 2s² 2p⁶ 3s² 3p⁶ 3d¹⁰] 4s², 4p⁶, and 5s² configuration with additional virtual 5p, 4d, 6s, 6p, 5d, 6d, 7s, and 7p Sturmian orbitals. The closed shells 1s²⋯3d¹⁰+1s²⋯3d¹⁰ form the core of the molecule and no excitations from core will be allowed. The 4s², 4p⁶, and 5s² orbitals are valence orbitals, and single and double excitations from these orbitals occur. Various covalent and ionic configurations are constructed by distributing electrons from the valence orbitals in all allowed ways over the 5p, 4d, 6s, 6p, 5d, 7s, and 7p

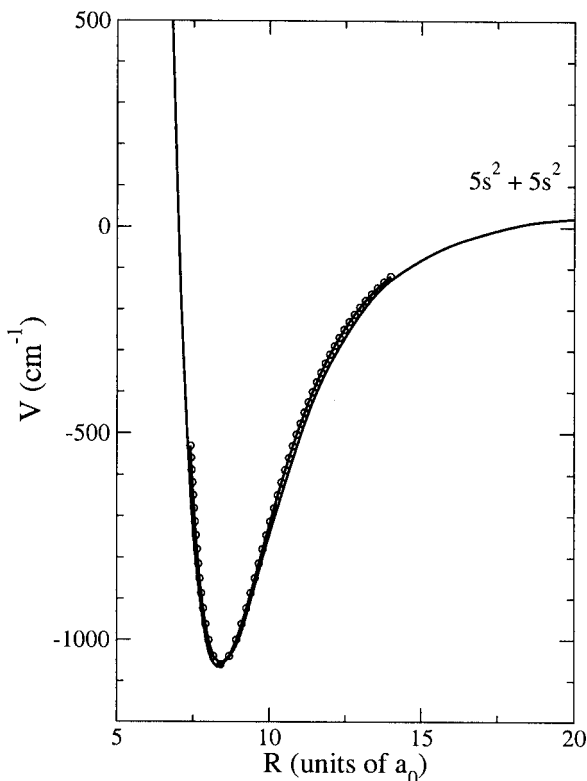


FIG. 1. The ground state $X^1\Sigma_g^+$ potential energy curve of Sr₂ as function of internuclear separation R . The solid line corresponds to the *ab initio* potential obtained in this study and the potential marked with circles is the RKR potential of Ref. 3.

orbitals. The number of molecular configurations in our basis set depends on the model. We have performed two types of calculations. The first type is aimed at calculating the best possible short- and intermediate-range potential by first perturbatively estimating the correlation of each molecular configuration with the ground state configuration. If the estimate falls below a threshold, this configuration is not included in the configuration interaction procedure. Inclusion of all configurations in the configuration interaction procedure is computationally prohibited. The second type of calculation gives the best possible long-range potential by excluding ionic configuration and switching off the exchange interaction and overlap integrals in the Hamiltonian in order to reduce the size of the matrix and to accelerate the calculation. The two calculations are combined at an internuclear separation between $18a_0$ and $20a_0$, because at these internuclear separations exchange and overlap is smaller than 1 cm^{-1} .

Figure 1 presents the ground state $X^1\Sigma_g^+$ potential of Sr₂ as a function of the internuclear separation R . The potential curve marked by circles is the RKR potential deduced from the experimental observations in Ref. 3. The solid line corresponds to the *ab initio* potential obtained in this study. Comparing our results with the RKR potential shows a good agreement. The ground state spectroscopic parameters are $D_e=1066\text{ cm}^{-1}$, $R_e=8.35a_0$, and $\omega_e=39.2\text{ cm}^{-1}$, whereas the experimental values of Ref. 3 are $D_e=1060\pm 30\text{ cm}^{-1}$, $R_e=8.40a_0$, and $\omega_e=40.32\text{ cm}^{-1}$. It appears that we selected a right set of atomic orbitals to describe the ground state potential.

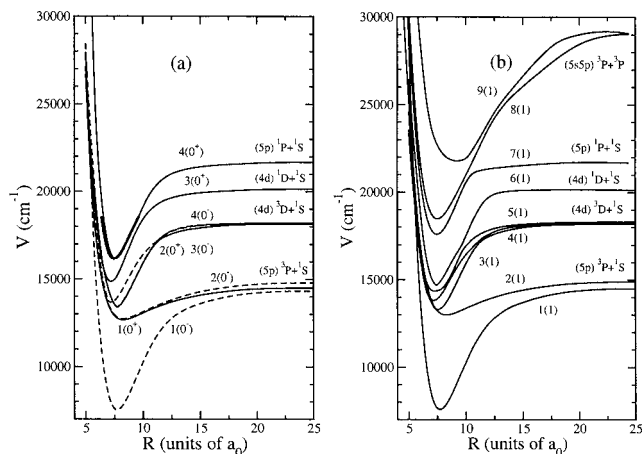


FIG. 2. Ungerade $\Omega=0^+$ (panel a) and $\Omega=1$ (panel b) relativistic potentials of Sr₂ dissociating to the $^1S+^3P$, $^1S+^3D$, $^1S+^1D$, $^1S+^1P$, and $^3P+^3P$ asymptotes. The RKR potential of the $A^1\Sigma_u^+(0_u^+)$ state is also shown in panel (a). In panel (a) we have not drawn the potentials dissociating to $^3P+^3P$ asymptotes. They are significantly less deep than those for $\Omega=1$ and show little mixing with potentials going to the lower limits. The zero of energy is located at the dissociation limit of the ground state of Sr₂.

The prominent feature of the first excited potentials of Sr₂ is the overlap between potentials dissociating to the $5s^2+5s5p$ and $5s^2+5s4d$ atomic limits. That is, the energies and thus the potentials dissociating to the $5s^2+5s4d$ limits lie between those of the $5s^2+5s5p$ limits. As a result of the overlap, there are several avoiding crossings between relativistic excited state potentials. This overlap is absent for the lighter alkaline-earth dimers. Therefore, for a correct modeling we have created a molecular basis set which includes $5s$, $5p$, and $4d$ orbitals equally accurate.

The closed shells $1s^22s^2\cdots 4s^2+1s^22s^2\cdots 4s^2$ form the core of the molecule and excitations from these shells are not allowed. The $4p^6$, $5s^2$, $5p$, and $4d$ orbitals are valence orbitals and single, double, and triple excitations are permitted. Unoccupied or virtual $5d$, $6s$, $6p$, $6d$, $7s$, $7p$, $7d$, $8s$, and $8p$ Sturmian orbitals are included in the basis set to treat correlation effects. Covalent and ionic configurations are constructed by distributing electrons from the valence orbitals in all allowed ways over both valence and virtual orbitals. The relativistic Hamiltonian is used and thus includes spin-orbit interactions between the excited nonrelativistic potentials.

In this study we have determined excited potentials with $\Omega=0$ and 1 ungerade symmetry since only they provide contributions to the ground state transition dipole moments and dynamic polarizability. The $\Omega=0$ and 1 potentials are presented in panels (a) and (b) of Fig. 2, respectively. Long-range potentials at large internuclear separations are constructed from the form $V(R)=D_e+C_3/R^3-C_6/R^6$. We used the recommended values of $C_3=-0.015074E_h a_0^3$ and $C_6=3513.8E_h a_0^6$ for the $1(0_u^+)$ state and $C_3=0.007537E_h a_0^3$ and $C_6=3773.85E_h a_0^6$ for the $1(1_u)$ state.¹⁵ For the higher excited $4(0_u^+)$ and $7(1_u)$ potentials we use $C_3=-18.36E_h a_0^3$ and $C_6=9.18E_h a_0^6$, respectively.⁸ All other dispersion parameter have been obtained by fitting continuously to our *ab initio* curves. We find $C_6=-1.7\times 10^5 E_h a_0^6$ for the $4(0_u^+)$ potential and $C_6=1.5\times 10^5 E_h a_0^6$ for the $7(1_u)$ potential. We matched

TABLE I. Equilibrium distance $R_e(a_0)$ and dissociation energy $D_e(\text{cm}^{-1})$ of the excited $\Omega=0_u^+$ and 1_u potentials of Sr_2 . The number n indicates the energy-ordered appearance of the potentials.

$n\Omega$	R_e	D_e	$n\Omega$	R_e	D_e
$1(0_u^-)$	7.8	6778	$1(1_u)$	7.8	6921
$1(0_u^+)$	8.2	1837	$2(1_u)$	8.2	1907
$2(0_u^-)$	8.2	2065	$3(1_u)$	7.4	4849
$2(0_u^+)$	7.8	4767	$4(1_u)$	7.2	4402
$3(0_u^-)$	7.4	4479	$5(1_u)$	7.0	3923
$3(0_u^+)$	7.2	5292	$6(1_u)$	7.4	5413
$4(0_u^-)$	7.2	4557	$7(1_u)$	7.42	4081
$4(0_u^+)$	7.61	5475	$8(1_u)$	7.6	10565
			$9(1_u)$	9.2	7272

our *ab initio* potentials to the long-range potentials between $20a_0$ and $30a_0$.

The zero of energy in Fig. 2 is located at the dissociation limit of the ground state of Sr_2 . At large internuclear separation the splittings between potentials are equal to the fine-structure splitting of the atomic P and D states. Panel (a) of Fig. 2 shows both 0_u^+ (solid lines) and 0_u^- (dashed lines) potentials for the completeness. However, the 0_u^- states cannot be accessed by spectroscopy from the ground state potential. The spectroscopic parameters D_e and R_e of the excited states are listed in Table I.

We have compared our calculation of the $4(0_u^+)$ potential dissociating to the $^1S_0+^1P_1$ asymptote with the RKR potential for the nonrelativistic $A^1\Sigma_u^+(0_u^+)$ state of Ref. 3. For short R this relativistic and nonrelativistic potentials coincide. The result of this comparison is shown in Fig. 2 (panel a). The spectroscopic constants of this potential available from the literature^{3,10,11} and our data are given in Table II. All calculated results in Table II are in good agreement with experiment.³ Our R_e , D_e , and ω_e values are slightly closer to the experimental data than results of other theoretical predictions, obtained within a nonrelativistic approximation.

Another excited potential observed in experiment⁴ is the $B^1\Pi_u$ potential. At short range this state corresponds to our relativistic $7(1)$ state shown in Fig. 2, panel (b). The spectroscopic constants of this potentials from all available sources are listed in Table II. Our D_e agrees with the theoretical

TABLE II. Comparison of spectroscopic parameters of the $4(0_u^+)$ and $7(1_u)$ states of Sr_2 with experimental (Refs. [3,4]) and other theoretical results (Refs. 10 and 11). At short range, the $4(0_u^+)$ and $7(1_u)$ states correlate with the $A^1\Sigma_u^+$ and $B^1\Pi_u$ states, respectively.

State	Source	$R_e(a_0)$	$D_e(\text{cm}^{-1})$	$T_e(\text{cm}^{-1})$	$\omega_e(\text{cm}^{-1})$
$A^1\Sigma_u^+$	Our data	7.61	5475	17269	88
	3	7.47	5400 ± 30	17357.9 ± 0.2	85.07
	10	7.75		17541	83
	11	7.47	5490	17280	80.21
$B^1\Pi_u$	Our data	7.42	4081	18658	72
	Ref. 4	7.28	590 ± 30	22173 ± 10	80.4 ± 1.0
	Ref. 10	7.47	16243	96	
	Ref. 11	6.75	4068		

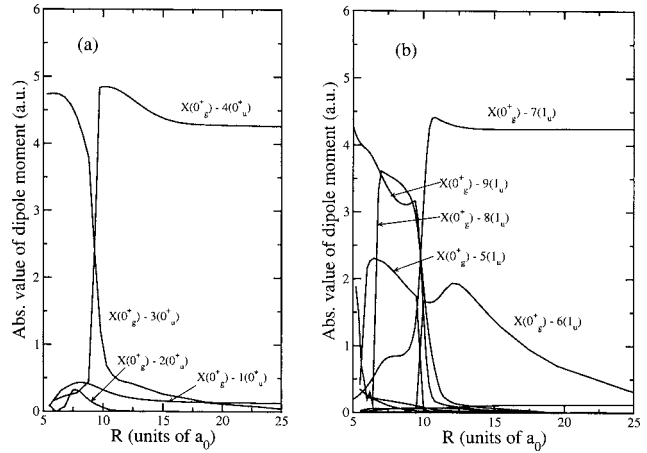


FIG. 3. Absolute value of transition dipole moments from the $X^1\Sigma^+$ ground state to excited states of $\Omega=0_u^+$ (panel a) and $\Omega=1_u$ (panel b) symmetries as a function of internuclear separation.

prediction of Ref. 11 while experimental potential depth obtained by Bordas *et al.*⁴ is seven times smaller. On the other hand our calculation agrees with the position of a potential minimum, R_e , provided in Refs. 4 and 10. We believe that the substantial disagreement between various theoretical predictions of spectroscopic constants of the $B^1\Pi_u$ state is a result of a different treatment of higher lying states dissociating to the $^3P+^3P$ limits, which might have significant interaction with the $B^1\Pi_u$ state.

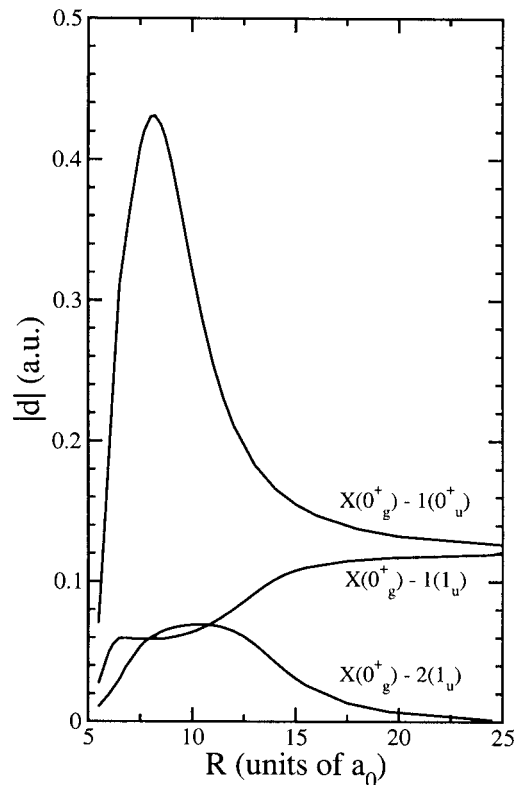


FIG. 4. Absolute value of transition dipole moments from the $X^1\Sigma^+$ ground state to excited states $1(0_u^+, 1_u)$ and $2(1_u)$ of Sr_2 .

IV. TRANSITION DIPOLE MOMENTS

The relativistic multiconfiguration molecular wavefunctions have also been used to calculate the transition electric-dipole moments between the $^1\Sigma^+$ state of the ground configuration and $\Omega=0_u^+$, 1_u components of excited potentials dissociating to the $5s+5p$, $5s+4d$, and $5s5p+5s5p$ limits. Absolute values of the nonzero transition dipole moments are shown in Fig. 3. At short-range internuclear separation the dipole moments strongly depend on R .

At long range of R , some transitions are strictly forbidden, but at short-range internuclear distances, they are allowed and have a significant rise mainly due to strong interaction with $^1\Sigma_u^+$ potential dissociating to $^1P+^1S$ limit. The sudden change in dipole moments in Fig. 3 (panel b) near $12.5a_0$ and $9.5a_0$ correlates with avoided crossings between the $\Omega=1_u$ components of the potentials dissociating to $^1P+^1S$ and $^3P+^3P$ limits and $^3D+^1S$ and $^1D+^1S$ limits, shown in Fig. 2. The singlet $X^1\Sigma^+$ to triplet $^3\Pi[1(0_u^+, 1_u)]$ transition dipole moments are 15–20 times smaller. We estimate that the uncertainty of the transition dipole moments is 5% based on a comparison of the dipole moments at $R=100a_0$ with the experimental dipole moments of the Sr atom.²¹ Figure 4 shows a blowup of the dipole moments presented in Fig. 3. It emphasizes the dipole moments to potentials dissociating to $^1S+^3P_{1,2}$ limits.

In conclusion, this paper has two main objectives. The first is to introduce a computational method capable of performing a fully *ab initio* relativistic calculation for a molecule with strong correlation effects. The second objective of this paper is to obtain detailed information about the electronic structure of the Sr₂ molecule relevant to ultracold experiments.

ACKNOWLEDGMENT

The author acknowledges the Army Research Office for support of this work.

- ¹T. Zelevinsky, S. Kotochigova, and J. Ye, "Precision test of mass ratio variations with lattice-confined untracold molecules," *Phys. Rev. Lett.* (to be published).
- ²T. Bergeman and P. F. Liao, *J. Chem. Phys.* **72**, 886 (1980).
- ³G. Gerber, R. Möller, and H. Schneider, *J. Chem. Phys.* **81**, 1538 (1984).
- ⁴C. Bordas, M. Broyer, J. Chevalerey, and Ph. Dugourd, *Chem. Phys. Lett.* **197**, 562 (1992).
- ⁵J. Stanton, *Phys. Rev. A* **49**, 1698 (1994).
- ⁶A. J. Sadlej and M. Urban, *J. Mol. Struct.* **234**, 147 (1991).
- ⁷S. G. Porsev and A. Derevianko, *Phys. Rev. A* **65**, 020701 (2002).
- ⁸M. Yasuda, T. Kishimoto, M. Takamoto, and H. Katori, *Phys. Rev. A* **73**, 011403 (2006).
- ⁹S. G. Porsev and A. Derevianko, *JETP* **102**, 195 (2006).
- ¹⁰N. Boutasseta, A. R. Allouche, and M. Aubert-Frecon, *Phys. Rev. A* **53**, 3845 (1996).
- ¹¹E. Czuchaj, M. Krosnicki, and H. Stoll, *Chem. Phys. Lett.* **371**, 401 (2003).
- ¹²T. P. Dinneen, K. R. Vogel, E. Arimondo, J. Hall, and A. Gallagher, *Phys. Rev. A* **59**, 1216 (1999).
- ¹³H. Katori, T. Ido, Y. Isoya, and M. Kuwata-Gonokami, *Phys. Rev. Lett.* **82**, 1116 (1999).
- ¹⁴P. G. Mickelson, Y. N. Martinez, A. D. Saenz, S. B. Nagel, Y. C. Chen, T. C. Killian, P. Pellgrini, and R. Cote, *Phys. Rev. Lett.* **95**, 223002 (2005).
- ¹⁵T. Zelevinsky, M. M. Boyd, A. D. Ludlow, T. Ido, J. Ye, R. Ciurylo, P. Naidon, and P. S. Julienne, *Phys. Rev. Lett.* **96**, 203201 (2006).
- ¹⁶See EPAPS Document No. E-JCPSA6-127-302747 for tables of the excited state potentials and transition dipole moments between the ground state and the excited states of the Sr₂ molecule. This document can be reached through a direct link in the online article's HTML reference section or via the EPAPS homepage (<http://www.aip.org/pubservs/epaps.html>).
- ¹⁷S. Kotochigova and E. Tiesinga, *J. Chem. Phys.* **123**, 174304 (2005).
- ¹⁸F. Grein and T. C. Chang, *Chem. Phys. Lett.* **12**, 44 (1971).
- ¹⁹J. H. Lenthe and G. G. Balint-Kurti, *J. Chem. Phys.* **78**, 5699 (1983).
- ²⁰R. Shepard, *Ab Initio Methods in Quantum Chemistry II*, edited by K. P. Lawley (John Wiley & Sons, New York, 1987), pp. 63–200.
- ²¹<http://physics.nist.gov/physrefdata/ASD>.